The isotopic composition of rainfall on a subtropical mountainous island

Giuseppe Torri[1], **Alison D. Nugent**[1], **Brian N. Popp**[2]

[1]Department of Atmospheric Sciences, University of Hawai'i at Mānoa, Honolulu, HI, 96822
[2]Department of Earth Sciences, University of Hawai'i at Mānoa, Honolulu, HI, 96822

Key Points:

- Significant leeward/windward differences in the rainfall isotopic composition due to differences in rain evaporation
- Deuterium excess shows seasonal variations due to different origin of air masses
- Isotope data show interannual variability that could be linked to large-scale modes of variability

Corresponding author: Giuseppe Torri, gtorri@hawaii.edu

Abstract

Tropical islands are simultaneously some of the most biodiverse and vulnerable places on Earth. Water resources help maintain the delicate balance on which the ecosystems and the population of tropical islands rely. Hydrogen and oxygen isotope analyses are a powerful tool in the study of the water cycle on tropical islands, although the scarcity of long-term and high-frequency data makes interpretation challenging. Here, a new dataset is presented based on weekly collection of rainfall H and O isotopic composition on the island of O‘ahu, Hawai‘i, beginning from July 2019 and still ongoing. Throughout this time, a variety of weather conditions have affected the island, each producing rainfall with different isotopic ratios: precipitation from Kona lows was found to have the lowest isotopic ratios, whereas trade-wind showers had the highest. These data also show some differences between the windward and the leeward side of the island, the latter being associated with higher rainfall isotope ratios due to increased rain evaporation. At all sites, the measured deuterium excess shows a marked seasonal cycle which is attributed to different origins of the air masses that are responsible for rainfall in the winter and summer months. The local meteoric water line is then determined and compared with similar lines for O‘ahu and other Hawaiian islands. Finally, a comparison is made with data collected on Hawai‘i Island for a longer period of time, and it is shown that the isotopic composition of rainfall exhibits significant interannual variability.

Plain Language Summary

Water molecules come in different forms that contain atoms of slightly different weights, called isotopes. Knowledge about the ratio of various isotopes in a water sample can be used to study past climates and the water cycle in a given region. Here, a new 2-year dataset of water isotopic composition is presented that was collected on the island of O‘ahu, in the Hawaiian Archipelago. By comparing the data with the weather conditions during each collection period, the isotopic signature of various weather systems is presented, and it is shown that large-scale storms, called Kona lows, produce rain that has particularly low heavy-to-light isotope ratios. Differences are also found between the isotopic composition of rain fallen on the windward side of the island and that on the leeward side, and this was attributed to differences in rain evaporation rates. A parameter called deuterium excess is computed, and its seasonal variations are interpreted as a result of differences in the origin of the air masses contributing to precipitating systems in winter and summer months. Finally, significant interannual differences were observed, suggesting a potential correlation with large-scale modes of climate variability, although a longer dataset will be needed to investigate this in detail.

1 Introduction

Climate represents an important component of the delicate equilibrium on which the biodiverse ecosystems on tropical islands rest (Veron et al., 2019). As the world begins to deal with the consequences of a changing climate, tropical islands are especially vulnerable to how those changes will manifest themselves at a regional scale (Veron et al., 2019). For example, in Hawai‘i more than 99% of the fresh water supply comes from rainfall (Gingerich & Oki, 2000). Any disruption to the hydroclimate in the North Pacific region can therefore threaten the ecosystems and the habitability of the islands, which are currently home to more than a million people (U.S. Census Bureau, 2020). A better understanding of the climate of tropical islands is therefore a task of utmost importance.

In the study of climate, analyses of the stable isotopic composition of water are a particularly useful tool. Because slight mass differences provide them with different chemical and physical properties (Dansgaard, 1964), δ^2H and δ^{18}O values in water can be used

to infer where an air parcel originated from, the climatic conditions at the origin, or the microphysical processes that it underwent in its history (Dansgaard, 1964; Galewsky et al., 2016). This has led to many important insights in disciplines, including, for example, paleoclimatology (Woodruff et al., 1981; Bar-Matthews et al., 1997; Cruz et al., 2005; LeGrande & Schmidt, 2009; Yao et al., 2013; Yoshimura, 2015; Kontakiotis, 2016; Opel et al., 2018; Cluett & Thomas, 2020) and ecology (Ehleringer & Dawson, 1992; Dawson et al., 2002; Marshall et al., 2007; Lai & Ehleringer, 2011; Cai et al., 2015; Evaristo et al., 2016; Grossiord et al., 2017; Lovelock et al., 2017; Aron et al., 2019; Adkison et al., 2020; Timofeeva et al., 2020; Hahn et al., 2021; Tetzlaff et al., 2021).

In Hawai‘i, stable isotopes in water have been used in a variety of different contexts. In recent years, measurements of the isotopic composition of water vapor at the summit of Mauna Loa, on Hawai‘i Island, have been used to diagnose important processes in the tropical atmosphere (Galewsky et al., 2007; Gupta et al., 2009; Noone et al., 2011; Hurley et al., 2012; Bailey et al., 2013; Galewsky, 2018). As another example, in the study of the islands' hydrology, the comparison between the isotopic composition of water found in springs and wells with that of rainfall has been used to determine flow paths and recharge areas for groundwater on different parts of Hawai‘i Island (Scholl et al., 1996; Tillman et al., 2014; Kelly & Glenn, 2015; Fackrell et al., 2020; Tachera et al., 2021), Maui (Scholl et al., 2002, 2007), and O‘ahu (Dores et al., 2020).

Most of the δ^2H and δ^{18}O values measured in water collected in Hawai‘i, however, are characterized by collection frequencies of the order of months. While these might be adequate to study processes involving groundwater aquifers, that occur over longer time scales compared to atmospheric phenomena, such long collection frequencies make interpretation of the data challenging. The longest available record of the isotopic composition of rainfall in Hawai‘i was collected with a monthly frequency between 1962 and 1970 as part of the Global Network of Isotopes in Precipitation (GNIP)(IAEA/WMO, 2021). However, the lack of reliable satellite data and the scarcity of other weather observations at the time make the interpretation of the isotope data equally challenging. The GNIP dataset also presented another limitation, because all the data were collected in a single location on the windward side of Hawai‘i Island, thus potentially introducing biases: for example, the same weather system coming from different directions would likely produce rain with different isotopic compositions thanks to the island orographic effect.

Here, a new dataset of δ^2H and δ^{18}O values of rainfall is presented. The data were collected on the island of O‘ahu with a weekly frequency over five different sites, two on the windward side and three on the leeward side. The data discussed here span two years, from July 2019 until July 2021, although collection is still ongoing. In Section 2, all the definitions and the data used for this study are introduced. In Section 3, the rainfall isotope dataset is presented and interpreted. In Section 4, the implications of the data are discussed. Finally, conclusions are presented in Section 5

2 Methods

2.1 Definitions

Throughout this manuscript, three stable water isotopologues are considered, $^1H_2{}^{16}O$, $^1H_2{}^{18}O$ and $^1H^2H^{18}O$. Isotopologues are referred to by the isotope that makes them different from the lighter isotopologue, $^1H_2{}^{16}O$: ^{18}O for $^1H_2{}^{18}O$ and ^2H for $^1H^2H^{18}O$. The isotope ratios of H and O are defined as the concentration of heavy isotope in a given sample divided by the concentration of the lighter isotope:

$$R_{^{18}\mathrm{O}} \equiv [^{18}\mathrm{O}]/[^{16}\mathrm{O}], \quad (1)$$

$$R_{^{2}\mathrm{H}} \equiv [^{2}\mathrm{H}]/[^{1}\mathrm{H}], \quad (2)$$

where the square brackets represent the concentration of an isotope. Isotope abundances are defined as

$$\delta X \equiv 1000 \times \left(\frac{R_X}{R_{VSMOW}} - 1 \right), \tag{3}$$

where R_{VSMOW} is the Vienna Standard Mean Ocean Water, and X indicates one of the two heavier isotopes. The unit of measurement for isotopic abundances is ‰, or permil.

From the isotopic abundances, a second-order parameter, called deuterium excess, d, can be defined as:

$$d \equiv \delta^2\mathrm{H} - 8 \times \delta^{18}\mathrm{O}. \tag{4}$$

Deuterium excess has been shown to be particularly sensitive to environmental conditions at the moisture source (Merlivat & Jouzel, 1979; Uemura et al., 2008; Pfahl & Sodemann, 2014), and it is thus often used as a diagnostic tool to investigate the origins of air masses responsible for precipitation in a particular region (Vimeux et al., 1999; Masson-Delmotte et al., 2005; Jouzel et al., 2007; Pfahl & Wernli, 2009; Pfahl & Sodemann, 2014).

The Global Meteoric Water Line (GMWL) is an empirical linear relationship between the H and O isotope abundances in water (Craig, 1961):

$$\delta^2\mathrm{H} = 8 \times \delta^{18}\mathrm{O} + 10‰. \tag{5}$$

While the GMWL was originally discovered by considering precipitation samples from all over the world, more regional versions have also been used (Rozanski et al., 1993). These, generally known as Local Meteoric Water Lines (LMWLs), represent the same empirical relationship, except that the slope and intercept of the lines can be different from the GMWL. Departures from the GMWL are typically linked to processes, like evaporation, that happen in a given region (Rozanski et al., 1993; Putman et al., 2019).

2.2 The Island of O‘ahu

O‘ahu is the third largest island of the Hawaiian Archipelago, a group of islands and islets that extends for thousands of kilometers in the North Pacific region. The surface area of O‘ahu covers approximately 1,544 km^2 and its topography has been shaped by two separate shield volcanos: the remnants of the northernmost one constitute the Ko‘olau Range, with a peak at 960 m called Pu‘u Kōnāhuanui; those of the southernmost volcano form the Wai‘anae Range, its highest peak being Mount Ka‘ala with an elevation of 1,220 m (*State of Hawaii Data Book*, 2004).

The climate of O‘ahu is divided in two main periods: a dry season, which, following other studies (Longman et al., 2021), is here defined as the 6-month window between May and October; and a wet season, that covers the remaining 6 months of the year. A quasi-permanent high-pressure center located thousands of kilometers northeast of the island strongly modulates its climate and is responsible for steady trade winds. These have been estimated to blow over the Hawaiian Archipelago 50-80% of the time during the wet season, and 85-95% during the dry season (Longman et al., 2021). The orographic lifting provided to the moist air flow by the Ko‘olau and the Wai‘anae ranges on O‘ahu causes cloud condensation and the formation of rain, most of which falls in the vicinity of the mountain ranges (Giambelluca et al., 2013).

Trade wind showers are not the only weather systems responsible for rainfall on O‘ahu (K. Kodama & Barnes, 1997; K. R. Kodama & Businger, 1998). During the wet season, a considerable amount of rainfall is often generated in relatively short periods of time by synoptic weather systems, such as cold fronts, upper-tropospheric troughs, and subtropical storms, called Kona lows (Simpson, 1952). Tropical cyclones (TCs) also contribute, although these typically occur during the dry season. In a recent study, Longman et al. (2021) analyzed daily rainfall on O‘ahu during the period 1990-2010 and determined

that non-disturbance type rainfall caused by trade winds accounted for 70.6% of the total rainfall amount during the 20-year window, cold fronts for 15.5%, Kona lows for 8.8%, upper-tropospheric lows for 3.6%, and TCs accounted only for 1.6%.

Interannual variability of rainfall in Hawai'i is driven mainly by two large-scale modes (Chu & Chen, 2005). The first is known as the El Niño Southern Oscillation (ENSO) and it happens on temporal scales between 2 and 8 years (Trenberth, 1997). Its positive phase, called El Niño, is characterized by an anomalous warming of the central/eastern parts of the tropical Pacific Ocean and a deepening of the Aleutian low. The second phenomenon is known as the Pacific Decadal Oscillation (PDO) (Mantua et al., 1997), and in its positive phase is characterized by colder sea surface temperatures (SSTs) in the Western Pacific Ocean, and warmer SSTs in the Central and Eastern Pacific Ocean. The PDO is characterized by longer frequencies than ENSO, single phases persisting sometimes over 20 years or longer. In Hawai'i, positive phases of ENSO tend to lead to lower rainfall amounts compared to the negative phases. Similarly, positive phases of the PDO are typically associated with drier conditions (Chu & Chen, 2005).

2.3 Data

2.3.1 Isotope sites

The rainwater collection network that was built to collect the data presented in this manuscript is made of five sites located on the island of O'ahu. The locations of the collection sites were chosen to give the network a northeast-southwest orientation. Because this is approximately the direction along which trade winds blow, the network makes it possible to look at the evolution of the isotopic composition of trade-wind showers as they move across the island and over the Ko'olau Range. Future expansions of the network are planned to include other locations on O'ahu as well as on other islands in the Hawaiian Archipelago.

On the windward side, the network is composed by two sites, one in the city of Kailua and the other in the residential district of Maunawili. On the leeward side, the site closest to the Ko'olau Range is at Lyon Arboretum, followed to the south by another site at the Hawai'i Institue of Geophysics (HIG) on the University of Hawai'i at Mānoa campus, and, finally, one in Waikīkī. A summary of the sites' names, positions, and deployment date is presented in Table 1. Collections of rainfall at Waikīkī, Lyon Arboretum, and HIG were made through a Palmex Rain Sampler 1, in which water enters through a cylinder measuring 13.5 cm in diameter and is deposited in a 3 L HDPE plastic bottle (Gröning et al., 2012). At Maunawili, collections were made through a Palmex Rain Sampler 2, which differs from the others only for its larger size and for the volume of the HDPE plastic bottles used (6/10 L instead of 3 L). In Kailua, rainfall was collected using a 1-L separatory funnel fitted with a 13.0 cm diameter funnel and filled with approximately 50 mL heavy mineral oil to prevent evaporation.

Restrictions put in place because of the COVID-19 pandemic–as well as concerns about our own safety–made some collections particularly challenging: Lyon Arboretum was closed to the public for several weeks in March and April 2020. Heavy precipitation that fell during those weeks caused the rain sampler to overflow, and the data are considered inaccurate. For similar reasons, data collection at Waikīkī was discontinued in March 2020, only a few months after the deployment of the rain sampler.

In addition to the collection in April 2020, there were a couple of other times when debris was found in the funnel of the rain sampler, which caused it to overflow. In turn, this could have affected the isotopic composition of the rain water: for example, the partial obstruction could have slowed down the flow of the water into the funnel, thus exposing it to additional evaporation when still in the funnel. While still reported in the figures in this manuscript, data from these collections are marked with crosses.

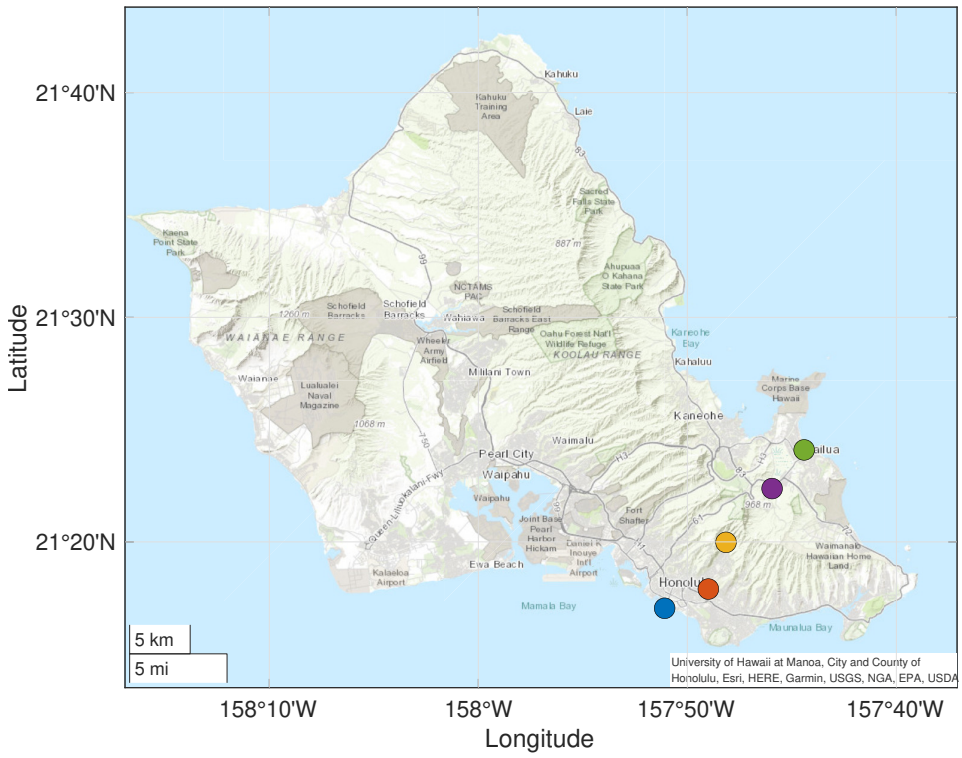

Figure 1. Topographic map of O'ahu with the five sites marked by colored circles: Kailua (green), Maunawili (purple), Lyon Arboretum (yellow), HIG (orange), and Waikīkī (blue).

Table 1. Summary of information relative to the sites deployed on O'ahu to collect the data used in this manuscript.

Site	Latitude	Longitude	Elevation	Deployment	Samples
Kailua	21º 24 '60" N	-157º 44' 25" E	8.5 m	07/06/2019 - current	110
Maunawili	21º 22' 22" N	-157º 45' 57" E	27.4 m	10/05/2019 - current	68
Lyon Arb.	21º 19' 59" N	-157º 48' 09" E	132.3 m	07/25/2019 - current	104
HIG	21º 17' 54" N	-157º 48' 60" E	40.8 m	09/28/2019 - current	81
Waikīkī	21º 17' 02" N	-157º 50' 29" E	2 m	10/04/2019 - 03/14/2020	13

Because the data was collected a little over two years, data from the Global Network of Isotopes in Precipitation (GNIP) are also considered to investigate interannual variability of rainfall isotopic composition in Hawai'i. GNIP is a network that was created in 1957 by the International Atomic Energy Agency and the World Meteorological Organization (IAEA/WMO, 2021). Sites were deployed in multiple locations throughout the entire world, and collections were typically done with a monthly frequency. In Hawai'i, only one GNIP site was deployed in Hilo, a town on the windward side of Hawai'i Island, and data were collected from 1962 until 1970.

2.3.2 Isotope analysis

Hydrogen and oxygen isotopic composition of rainwater was determined using cavity ring-down spectroscopy (a L2130-I, Picarro) equipped with a high-precision vaporizer (V1102-I, Picarro, Inc., Santa Clara, CA, USA) and autosampler (HTC PAL, Leap Technologies, Carrboro, NC, USA) with Chem-Correct acquisition software that monitors for interference of isotopologues of water by organic compounds (Gupta et al., 2009). All measurements were performed in the nitrogen carrier mode, using ultra-high-purity nitrogen (< 10 ppm H_2O, $> 99.99\%$ N_2; ALPHAGAZ1, Air Liquide, Houston, TX, USA). Samples were normalized to VSMOW using results of analysis of at least three laboratory reference materials that were extensively calibrated with NIST reference materials and had δ^2H and δ^{18}O values that bracketed the values of all samples. These laboratory reference waters were analyzed so that they bookended every 8 to 14 unknowns. Based on repeated measurements of an internal laboratory reference water similarly calibrated using NIST reference material and analyzed as an unknown, the precision for this method was less than $\pm 0.05‰$ for δ^{18}O values and $\pm 0.5‰$ for δ^2H values.

2.3.3 Weather data at Lyon Arboretum and HIG

Hourly rainfall data from HIG were collected using a Campbell Scientific TE525WS Texas Electronics Tipping Gauge (8" orifice), whereas hourly relative humidity data were collected using a Campbell Scientific EE181-L Air Temperature and Relative Humidity sensor. The former has accuracy of $\pm 1\%$ at rates up to 1 inch/hour, whereas the latter has accuracy of $\pm 1.3\%$ for temperatures and relative humidities typically found on O'ahu. The data cover a time interval between 16 October 2019 and 27 August 2021.

Rainfall and relative humidity data from Lyon Arboretum were collected at a 15-minute frequency using a CR3000 Campbell Scientific data logger and associated sensors (HUMICAP 180R sensor for relative humidity). In order for rainfall data to be directly comparable with those from HIG, they were converted into hourly with a simple accumulation sum. For typical conditions at Lyon Arboretum, the accuracy of the humidity sensor is $\pm 1\%$, whereas for the rain gauge it is $\pm 1\%$ up to 2 inches/hour of rain. Both rainfall and relative humidity data at Lyon Arboretum cover a period from 23 February 2018 until 26 April 2021.

When comparing datasets from HIG and Lyon Arboretum, an intersection of the two distinct temporal windows (16 October 2019 - 26 April 2021) is considered to select the data.

2.3.4 HYSPLIT

In order to diagnose the origin of air parcels flowing over O'ahu, the NOAA Air Resources Laboratory's Hybrid Single Particle Lagrangian Integrated Trajectory (HYSPLIT) model, version 5.1.0 for Linux, was used (Draxler & Hess, 1998; Stein et al., 2015). The model uses meteorological data to compute the forward/backward transport and dispersion of a tracer or of a number of trajectories. It is extensively used in the study

of atmospheric processes, with applications including transport of pollutants, allergens, or volcanic ash (Stein et al., 2015).

Following similar approaches (Sodemann et al., 2008; Barras & Simmonds, 2009; Guan et al., 2013; Aemisegger et al., 2014; Papritz et al., 2021; Villiger et al., 2021; Dahinden et al., 2021), HYSPLIT was used to interpret the deuterium excess data. First, a temporal window of 24 months, from 01 July 2019 until 30 June 2021 was selected. This choice was made in order to maximize the overlap with the collected isotope data and also to maintain a symmetry between the number of wet- and dry-season months considered. Then, for each day during the time window, 27 trajectories were initialized at a point with the same latitude-longitude coordinates as Lyon Arboretum at an altitude of 500 m, and their positions were integrated backward in time for 5 days. The integration was conducted using meteorological data from ERA5 reanalysis (Hersbach et al., 2019).

The choice of initializing the trajectories at 500 m was made to ensure that the calculation would capture air parcels that are most likely to contribute to rainfall on O‘ahu: because of the trade-wind inversion that persists at an altitude of approximately 2-2.5 km for most of the year (Cao et al., 2007), parcels in the free troposphere are unlikely to contribute often, except during precipitation from synoptic systems. Sensitivity tests were conducted by initializing trajectories at 2,500 m and at 5,000 m, but the conclusions reached were qualitatively the same. Sensitivity tests were also conducted by only considering trajectories initialized in periods when rainfall was collected at Lyon Arboretum, but no qualitative difference was noticed.

3 Results

3.1 Rainfall

For the collection period discussed here, the time series of rainfall rates observed at each site are presented in Figure 2a.The rates are computed by dividing the amount of water collected at each sampling period by the number of days over which the collection took place (Giambelluca et al., 2013). As expected, the figure shows that the highest rain rates were recorded during the wet season, between the months of October and April. These peaks are typically due to Kona lows, like those in March 2020 and 2021, or cold fronts affecting the islands, responsible for the peaks observed in mid-to-late December and January 2019, or the local maximum observed in early February 2021, which led to the formation of a number of deep convective storms on O‘ahu.

The dry season tends to be characterized by lower rain rates, mostly due to trade wind showers. Occasionally, TCs and tropical storms (TSs) can affect the Hawaiian Islands during the dry season. During the collection period, 4 TC/TS events were recorded. First, on 8 July 2019, the remnants of TC Barbara passed south of the islands and brought rainfall to the islands, especially on the windward side. Following that, the remnants of TC Erik and Flossie also affected Hawai‘i on 12 and 16 July 2019, respectively. Although, as will be seen later, rainfall from these three systems had a different isotopic composition compared to trade-wind showers, the rainfall rates were not significantly higher. The following year, TC Douglas passed remarkably close to the Hawaiian Islands around 25 July 2020. Enhanced rainfall rates by Douglas can be seen in Figure 2a, especially for the Kailua and the Lyon Arboretum site.

Another important feature shown by Figure 2a is that significantly more rainfall is often collected at Lyon Arboretum than all the other sites. For example, as can be inferred from Figure 2b, the median rain rate at Lyon Arboretum is 8.03 mm day^{-1}, whereas at HIG, only 4 km downwind, it is 1.35 mm day^{-1}, which is comparable to the median rate rate recorded at the other sites. Considering the location of the Lyon Arboretum

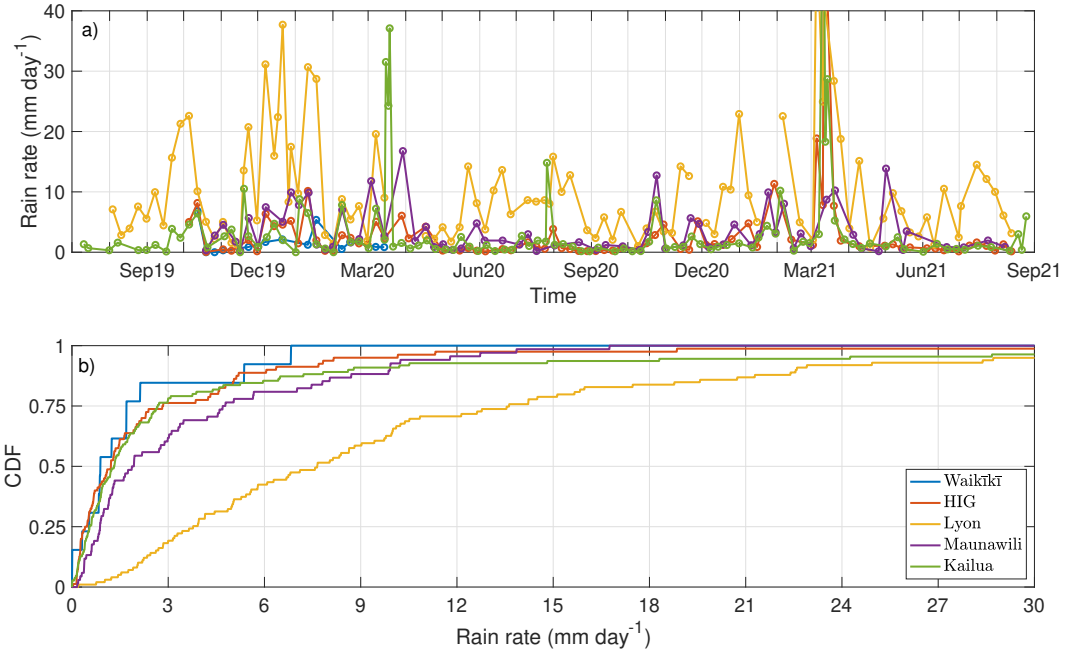

Figure 2. a) Time series of rain rates for the five sites, determined as the total accumulated rain for each collection period divided by the time since the previous collection. b) Cumulative distribution functions of rain rates.

rain collector, this can easily be explained as due to orographic enhancement provided by the Koʻolau mountains.

3.2 Rainfall ^{2}H and ^{18}O isotopic composition

The time series of δ^2H and δ^{18}O values for the five deployed sites are shown in Figure 3a and 3b, respectively. Precipitation from two Kona lows (March 2020 and 2021) has the lowest δ^{18}O and values of all the collection period, with particularly low δ^2H values ($\sim$ 64.0‰) recorded at the Kailua station. Rainfall from TCs, or their remnants, also appear to have low δ^2H and δ^{18}O values, although not as low as Kona lows (δ^2H $\sim$ -32.0‰). A low pressure system to the north of the islands on 10-11 October 2019 led to the advection of moist flow from the southeast, which ultimately resulted in a series of thunderstorms that produced very low δ^2H values (~ -52.6‰ at the Waikīkī site). Thunderstorms were also observed during other periods, for example on 18-19 November 2019 and on 3 February 2021, but the rainfall they produced did not have particularly low values of δ^2H and δ^{18}O.

Figure 4a shows the times series of δ^{18}O values of rainfall as a function of the average rain rate during each collection period (δ^2H values look very similar but is not shown). Because Lyon Arboretum is characterized by larger rain rates than any other site, and given that the sites have similar distribution functions of rain rates (Figure 2b), the data are presented as a function of rain rate percentiles. Rainfall, particularly during the dry season (Figure 4c), appears to have a remarkably consistent isotopic composition, although, as Figure 2b illustrates, the bottom 75 percentiles correspond to relatively small rain rates, especially for leeward sites. Nevertheless, for those rain rates, rainfall collected at HIG tends to be enriched in ^{18}O by 1-1.5 ‰ than at any other site.

In order to gain a more quantitative understanding of the isotopic composition of rainfall collected, and in order to compare the data with similar datasets on Oʻahu, a

Figure 3. Time series of δ^{18}O (a) and δ^{2}H (b) values for the five sites: Kailua (green); Maunawili (purple); Lyon Arboretum (yellow); HIG (orange); Waikīkī (blue). Black crosses represent data collected when the sampler had overflown.

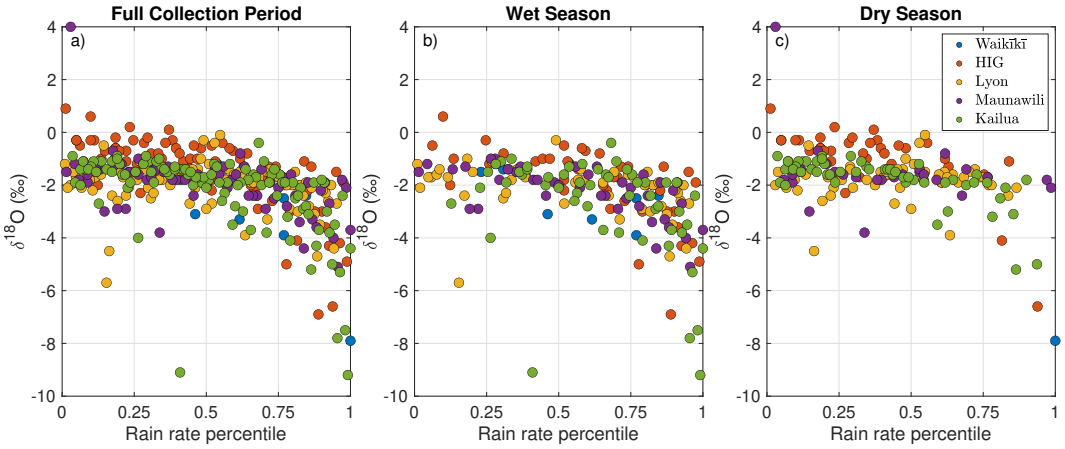

Figure 4. δ^{18}O values as a function of rain rate percentile for each site shown for the entire collection period (a), only considering wet-season rainfall (b), and only considering dry-season rain (c).

Table 2. Volume-weighted averages of δ^{18}O and δ^{2}H values and deuterium excess for the five sites computed considering all the collection period (1st, 4th, and 7th rows), only the wet seasons (2nd, 5th, and 8th rows), and only the dry season (3rd, 6th, and 9th rows). Numbers in parentheses represent standard errors associated with the mean values.

	Waikīkī	HIG	Lyon Arb.	Maunawili	Kailua
δ^2H_{tot}(‰)	-19.39 (5.81)	-11.56 (1.57)	-3.99 (0.67)	-7.99 (1.10)	-14.57 (1.83)
δ^2H_{wet}(‰)	-8.93 (1.78)	-12.44 (2.10)	-4.89 (1.13)	-10.30 (1.44)	-18.16 (2.84)
δ^2H_{dry}(‰)	-52.60	-8.51 (2.49)	-2.92 (0.63)	-1.67 (0.86)	-6.53 (1.26)
$\delta^{18}O_{tot}$(‰)	-3.79 (0.73)	-2.85 (0.20)	-2.10 (0.09)	-2.63 (0.13)	-3.32 (0.21)
$\delta^{18}O_{wet}$(‰)	-2.50 (0.27)	-3.02 (0.26)	-2.38 (0.13)	-2.94 (0.16)	-3.77 (0.33)
$\delta^{18}O_{dry}$(‰)	-7.90	-2.26 (0.35)	-1.75 (0.09)	-1.77 (0.11)	-2.30 (0.16)
d_{tot}(‰)	10.93 (0.73)	11.23 (0.29)	12.78 (0.32)	13.04 (0.32)	11.97 (0.30)
d_{wet}(‰)	11.04 (0.87)	11.71 (0.37)	14.18 (0.46)	13.25 (0.40)	12.01 (0.46)
d_{dry}(‰)	10.60	9.61 (0.42)	11.11 (0.33)	12.46 (0.52)	11.88 (0.28)

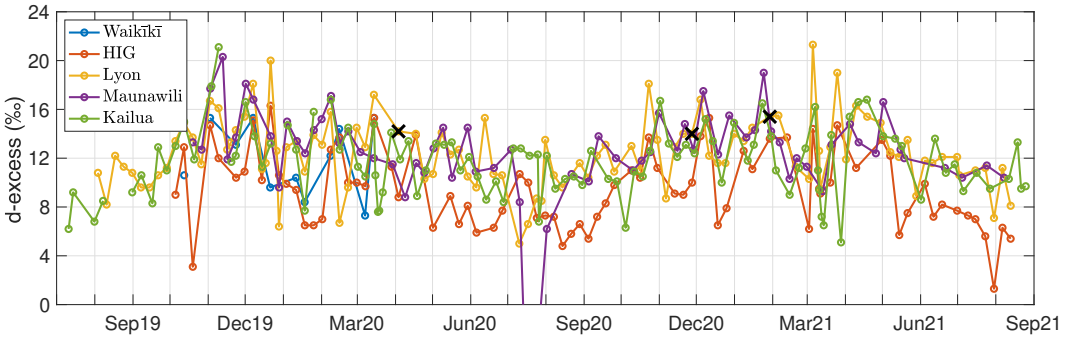

Figure 5. Time series of deuterium excess for each site during the entire collection period, from July 2019 to August 2021. The colors of the time series are the same as Figure 3. Black crosses represent data collected when the sampler had overflown.

summary of the volume-weighted averages of isotopic abundances for each site is given in Table 2.

3.3 Deuterium excess

The time series of deuterium excess derived from Equation 4 for the five sites is presented in Figure 5. The figure presents two interesting features. The first is the apparent seasonal cycle, with higher deuterium excess during the wet season and lower values during the dry season, and a difference between the two of approximately 5 ‰. This phenomenon has been observed both on a global scale (Araguás-Araguás et al., 2000; Pfahl & Sodemann, 2014) and at a regional level in other locations (Delmotte et al., 2000; Yoshimura & Ichiyanagi, 2009; Guan et al., 2013; Kopec et al., 2019). Because deuterium excess has been shown to be sensitive to relative humidity and SST at the moisture source (Merlivat & Jouzel, 1979; Uemura et al., 2008; Pfahl & Sodemann, 2014), changes in the environmental conditions at the source, or the presence of difference sources, are typ-

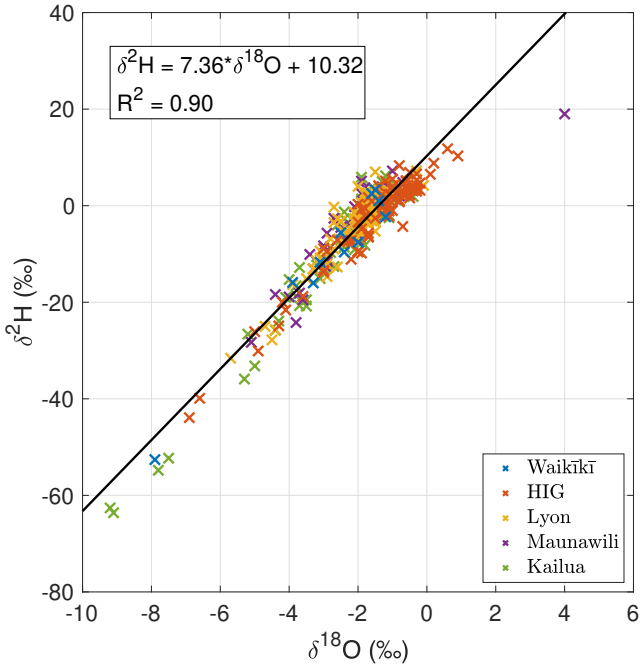

Figure 6. LMWL (black line) diagnosed from a linear regression of all the data from the five sites (colored crosses) over the entire collection period. The slope and the intercept of the linear regression, as well as the R^2 are reported in the top-left corner.

ically used to explain seasonal changes to deuterium excess values. Another interesting feature in Figure 5 is that, particularly during the dry season, the HIG site has consistently lower deuterium excess compared to other sites. A more quantitative comparison of the deuterium excess values measured at the five sites is presented in the last three rows of Table 2, which represent the volume-weighted averages for the entire collection period, for the wet season and for the dry season only.

3.4 The Local Meteoric Water Line

The black line in Figure 6 represents the LMWL for O‘ahu determined using a linear regression based on all the data collected (shown in colored crosses). While most data points seem to align relatively well with the LMWL, data at the extremes–either very low or very high values of δ^2H and δ^{18}O–appear to lie under the LMWL, potentially an indication of sub-cloud rain evaporation. The slope and the intercept of the LMWL are reported in Table 3.

As a way to test the sensitivity of the LMWL to the geography of the network and the temporal window over which the collection is conducted, Table 3 also reports results from a simple experiment. The second and third row are obtained by first subdividing the sites into those on the windward side of the island (Kailua and Maunawili) and those on the leeward side (Lyon Arboretum, HIG, and Waikīkī). The fourth and the last row contain results from regressions conducted using all data from 01 July 2019 until 30 June 2020, and from 01 July 2020 until 30 June 2021, respectively. The results show considerable variability, which naturally raises the question of what spatial and temporal scales must be taken into consideration in order to determine a LMWL which is representative of O‘ahu and, more generally, the Hawaiian Archipelago.

Table 3. Slopes and intercepts of LMWL computed using the entire dataset (1st row), considering only the sites on the windward side (2nd row), those on the leewardside (3rd row), or only data during the first or the second collection year (4th and 5th rows, respectively). The last row contains the slope and the intercept of the LMWL determined by Dores et al. (2020). Numbers in parentheses represent standard deviations.

	Slope (‰/‰)	Intercept (‰)
Total	7.36 (0.13)	10.32 (0.30)
Windward	7.70 (0.18)	11.44 (0.46)
Leeward	7.02 (0.18)	9.34 (0.40)
Year 1	7.77 (0.16)	11.49 (0.42)
Year 2	6.89 (0.20)	9.21 (0.43)
Dores et al. (2020)	7.22	10.31

4 Discussion

Although the hydrogen and oxygen isotopic composition of water has been used in many different areas within the study of climate, an incomplete understanding of how various atmospheric processes affect the isotopic composition of precipitation contributes to making the interpretation of records difficult. While numerical models can be a key to progress, the relative lack of long-term high-frequency time series of δ^2H and δ^{18}O values can be a hindrance to this progress. This study contributes to the current debate by introducing a new dataset of rainfall isotopic composition on the Island of O‘ahu. Compared to other collections conducted in the Hawaiian Islands in the past decades, this dataset has a much higher temporal resolution and, at the same time, it also includes multiple sites spread across a mountainous range on the island.

4.1 Rainfall isotopic composition

Even though they were collected at different frequencies and over different time periods, the data presented in this work compare favorably with those discussed in Dores et al. (2020). In particular, in almost all sites, rainfall appears to be be characterized by lower values of δ^2H and δ^{18}O during the wet season than the dry season, something that had been noticed by collections on the other islands as well (Scholl et al., 1996, 2002, 2007; Tillman et al., 2014; Kelly & Glenn, 2015; Fackrell et al., 2020; Tachera et al., 2021). One advantage of the data discussed here, however, is that the increased temporal resolution gives a clearer picture of the isotopic composition of rainfall due to different types of synoptic systems or weather disturbances. For example, Figure 3 revealed that Kona lows, subtropical storms that happen during the wet season can generate precipitation with, for example, δ^2H values as low as -64‰. Other precipitating systems, like cold fronts or thunderstorms were also associated with low δ^2H and δ^{18}O values, but not as much as Kona lows. The differences in the rainfall isotopic composition of various weather systems and their seasonality might also explain why wet-season isotopic compositions appear to be characterized by greater variability than dry-season ones (Figures 3a and b).

A series of recent works presented reconstructions of precipitation δ^2H values obtained from peatlands on Moloka‘i (Beilman et al., 2019) and O‘ahu (Massa et al., 2021) over the last 12 ka and 45 ka before present (BP), respectively. The data show periods characterized by low δ^2H values of peatland water—e.g., 3 ka and 9-10 BP—interspersed

by longer periods of comparatively higher values. The authors interpreted the low values as suggestive of an increased activity of Kona lows and cold fronts during those time intervals. Apart from providing support to this interpretation, the dataset presented in this manuscript also suggests that rainfall from Kona lows presents lower δ^2H values than that from cold fronts. Taken together, these results could imply that low δ^2H values in peatland water might be a reflection of changes in Kona low activity, as changes in cold front and extratropical storm activity would be unlikely to leave a strong isotopic signature in the paleorecord. On such long time scales, however, other factors might also play a role: for example, changes in vegetation cover might lead to greater evapotranspiration rates, which could affect the rainfall isotopic composition (Scholl et al., 2007). A detailed analysis of this is beyond the scope of this manuscript and is left for future work.

The dataset presented in this manuscript also allows an assessment of the spatial variability of rainfall δ^2H and δ^{18}O values. Considering that the climate in the Hawaiian Islands is dominated by trade winds, which blow with an easterly/northeasterly direction, a reasonable a priori expectation would be that rainfall collected on the windward side of the island is more enriched in ^{2}H and ^{18}O that that on the leeward side: as the air flow is lifted by the island orography, water vapor first condenses and then precipitation forms; as clouds continue their journey across the island, progressive rainout leads to lower δ^2H and δ^{18}O values in rainfall. The data presented here, however, paint a more complex picture.

While Figure 3 and Table 2 suggest that ^{2}H and ^{18}O abundances at the Waikīkī site are generally lower than at the Kailua site, particularly during the dry season, δ^2H and δ^{18}O values seem to progressively increase as the air flows over the Koʻolau Range and then decrease again as it flows past the mountains. As Figure 2b shows, the sites at Maunawili and Lyon tend to have higher precipitation rates than other sites (Giambelluca et al., 2013), so that one might expect δ^2H and δ^{18}O values to be lower there (Dansgaard, 1964).

One hypothesis to explain this apparent paradox, at least in part, is that different weather systems affect the five sites in different ways, due to their different windward and leeward locations across the Koʻolau Mountain Range, and they do not necessarily bring rainfall in proportional amounts to the five sites. For example, cold fronts and Kona lows, which are associated with low values of δ^2H and δ^{18}O, have a size and an intensity that likely affects the entire island of Oʻahu, or at least substantial portions of it. On the other hand, trade-wind showers, which tend to have comparatively higher values of δ^2H and δ^{18}O than Kona low rainfall, are largely caused by the orographic lifting provided by the Koʻolau mountains. Because of the easterly/northeasterly direction of the winds, trade-wind showers are likely to lead to large amounts of rain on the summits and immediately downwind of the mountains, where Lyon Arboretum is located. However, since the orographic forcing ceases after passing the mountain summits, many of these showers stop before reaching the HIG site. Thus, trade-wind showers affect Lyon Arboretum disproportionately compared to the rest of the network and cause the volume-weighted average to be higher than other places.

To check the consistency of this hypothesis, the daily accumulated rainfall at HIG is matched with the daily accumulated rainfall at Lyon Arboretum, and the result is presented in Figure 7a. If HIG is receiving only proportionately less rainfall for each event affecting Lyon Arboretum, one would expect a good correlation between the daily accumulated rainfall at both sites. Instead, rainfall appears not particularly correlated, and there seem to be many days when rainfall is recorded at Lyon Arboretum but not at HIG, particularly during the dry season, where rainfall is mostly due to trade-wind showers.

Figure 7b shows the cumulative distribution function of daily accumulated rainfall at HIG for days when more than 0.5 mm of rain was collected at Lyon Arboretum.

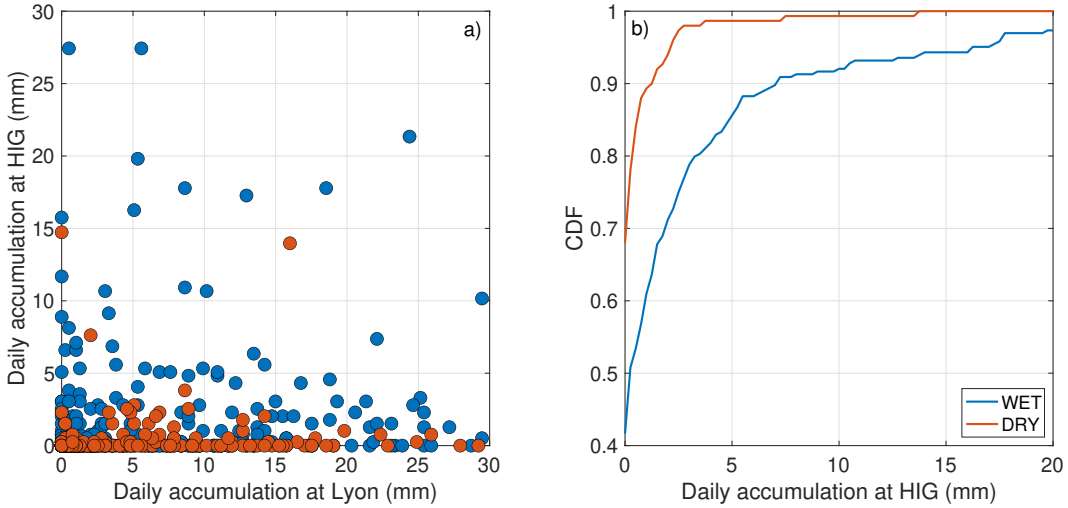

Figure 7. a) Daily accumulated rainfall at HIG shown as a function of rainfall accumulated at Lyon Arboretum for the same day. b) Cumulative distribution function of daily accumulated rainfall at HIG for days during the wet (blue) and dry (red) season when more than 0.5 mm of rain was collected at Lyon Arboretum.

The curves show that, for 41.5% of those days during the wet season and for 68.0% during the dry season, no rainfall was collected at HIG in spite of some being recorded at Lyon Arboretum. The numbers increase when attention is restricted to days with small amounts of precipitation at Lyon Arboretum that do not exceed 5 mm (53.3% during the wet season and 72.6% during the dry season; not shown).

Differences in precipitation frequency due to the orographic effect might partially explain the values of ^{2}H and ^{18}O isotope abundances observed in Table 2, although other factors could also contribute. For example, Figures 3 and 4 suggest that in many events, particularly during dry seasons, rainfall at the HIG site had higher δ^{2}H and δ^{18}O values than other stations. Furthermore, Figure 5 shows that, for those events, rainfall at HIG also has lower deuterium excess than other stations. It is hypothesized that these differences can be explained in terms of rain evaporation. Figure 8 represents the diurnal cycle of the average relative humidity at Lyon Arboretum (yellow) and HIG (purple). The figure shows a differences between the relative humidity at Lyon Arboretum and HIG of the order of 10%, which supports the hypothesis that rain collected at the latter site experiences significant amounts of rain evaporation. This is perhaps not surprising considering that Lyon Arboretum is at the back of the Mānoa Valley and is surrounded by vegetation, whereas HIG is in a more urban setting. The sharp gradient of relative humidity in a relatively short space is an illustration of strong variability of microclimates on the Hawaiian Islands. During rain evaporation, kinetic fractionation leads to an enrichment of rainfall ^{2}H and ^{18}O isotopes and to lower values of deuterium excess.

A close examination of the data also suggests that rainfall δ^{2}H and δ^{18}O values are higher at the Maunawili site, on the windward side but close to the Koʻolau Range, than at Kailua, also on the windward side but farther away from the mountains and closer to the ocean. Deuterium excess is also higher in precipitation in Maunawili than in Kailua. As argued by Scholl et al. (2007) when interpreting differences between windward and leeward rainfall isotopic composition on Maui, it is possible that a higher abundances and higher deuterium excess might indicate that air flowing over the island entrains water vapor that has been evapotranspired from the local vegetation (a processed they re-

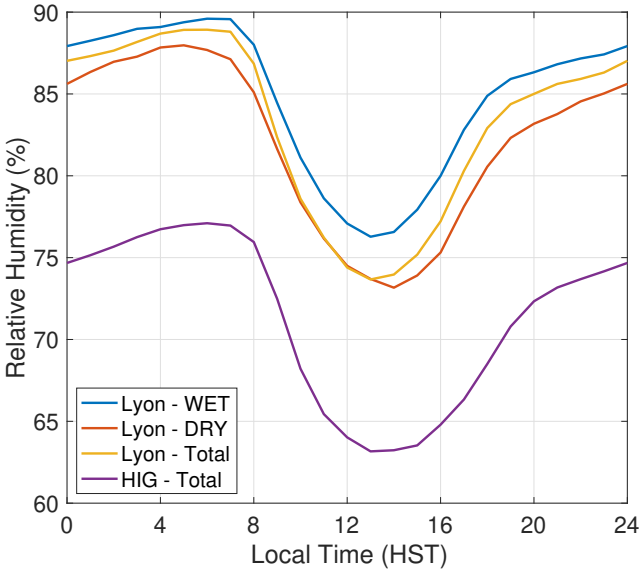

Figure 8. Average diurnal cycles of relative humidity at Lyon Arboretum for the entire period (yellow), for the wet (blue) and the dry (red) season only, and at HIG for the entire period (purple).

ferred to as "recycling"). Unfortunately, using rainfall ^{2}H and ^{18}O abundances alone, it is hard to draw any definitive conclusion. A follow-up paper is in preparation in which isotope-enabled cloud resolving models are used precisely to address these types of questions.

Another important point that emerges from the systematic differences observed in the dataset, as well as with other extended network of sites in Hawai'i (Scholl et al., 2007; Dores et al., 2020), is that caution should be taken when using data from single sites in locations with complex topography. In the case of Hawai'i, for example, GNIP collected many years of data in a single location in Hilo, on the windward side of Hawai'i Island. If indeed, as suggested by Scholl et al. (2007) for Maui, windward locations experience stronger water vapor recycling in the presence of significant topography, isotope data in Hilo might have systematically lower δ^{2}H and δ^{18}O values and higher deuterium excess than rainfall over the open ocean.

4.2 Deuterium excess and moisture origin

As briefly discussed in Section 3.3, the deuterium excess values shown in Figure 5 present seasonal variations at all the sites. Consistent with other observations across the planet (Araguás-Araguás et al., 2000; Delmotte et al., 2000; Yoshimura & Ichiyanagi, 2009; Guan et al., 2013; Pfahl & Sodemann, 2014; Kopec et al., 2019), this behaviour for data in Hawai'i is hypothesized to be due to changes in the air masses that contribute to precipitation at different times of the year: while synoptic systems that are responsible for much of the rainfall during the wet season originate in the Northwestern Pacific (K. Kodama & Barnes, 1997; K. R. Kodama & Businger, 1998), rainfall during the dry season is mostly due to the trade-wind flow, which originates in the Northeastern part of the Pacific basin.

In order to assess the consistency of this hypothesis, the backward trajectories generated with HYSPLIT (see Section 2.3.4) are considered. First, the trajectories are divided in those initiated during the wet season and those during the dry season. Then,

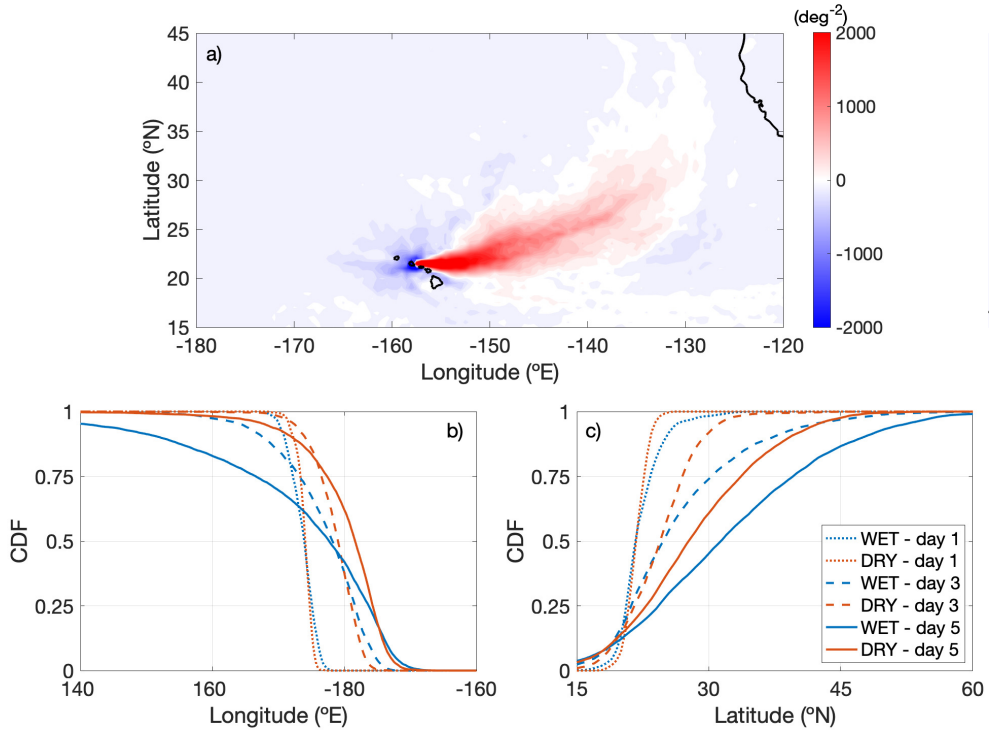

Figure 9. a) Differences in trajectory densities between dry- and wet-season months; Cumulative distribution function of longitude (b) and latitude (c) coordinates for trajectories during the wet (blue) and dry (red) season at 1 (dotted), 3 (dashed), and 5 (continuous) days prior to their initialization.

histograms are derived based on the latitude and longitude of each trajectory at any point in its history. The difference between the histogram for the dry season and that for the wet season is shown in Figure 9a. The plot shows that, during the dry season, trajectories tend to have a more coherent north-eastern origin, which is consistent with trade winds being more prevalent during this time of year. During the wet season, many trajectories still originate from the high-pressure area to the north-east of O'ahu, although a considerable number of trajectories originate to the west and to the north of the island.

In order to quantify these differences, the cumulative distribution function of particles' longitudes at different times during the wet season (blue) and the dry season (red) is shown in Figure 9b. The figure suggests that, five days ahead of the particles' initiation time, there is a difference of 21.5^{o} in longitude of the 75th percentile of the distribution for the wet and the dry season trajectories. Figure 9c shows a difference of 6^{o} for the 75th percentiles of wet and dry season trajectories.

Considering the differences between SST and relative humidity in the Central and West Pacific during the winter months and those in the Eastern Pacific during the summer months (see, e.g., Figure 2 of Pfahl and Sodemann (2014)), the analysis above supports the hypothesis that differences in the moisture sources contributing to the precipitating events of the wet and dry season could help explain the seasonal changes in deuterium excess observed.

This suggests a connection between the deuterium excess found in rainfall in Hawai'i and the large-scale dynamics that influence the climate in the North Pacific region. In

principle, this connection could be used to diagnose, or at least provide further constraints on those dynamics at times for which there was insufficient coverage of meteorological data, for example when the GNIP site in Hilo was active, or in the interpretation of paleoclimate data, assuming that both δ^{18}O and δ^{2}H values are available.

On a more local scale, another potential contributing factor that would lead to seasonal changes of deuterium excess are differences in rain evaporation that precipitating columns experience in different seasons. The blue and red curves in Figure 8 the diurnal cycle of the average relative humidity at Lyon Arboretum during the wet and the dry season, respectively. In spite of the similarities between the two curves, relative humidity values during the dry season are lower than the wet-season curve by 4-5%. This is particularly evident in the afternoon/evening, when a peak in rainfall from trade-wind showers is often observed in many locations across the island (Hartley & Chen, 2010). Assuming that the spectrum of raindrops does not vary too much throughout the year, rain that falls during the dry season should experience more rain evaporation.

4.3 Interannual variability

In Section 3.4, the LMWL computed from the network of sites was presented. Even though the network used here covers a much smaller area than the network used by Dores et al. (2020), the LMWLs are comparable. However, as also highlighted by Dores et al. (2020), considering all the isotope collections that have been made in Hawai‘i, some important differences emerge. For example, from a 2-year collection conducted on East Maui, Scholl et al. (2002) computed a LMWL with slope and intercept of 8.2 ‰/‰ and 14.7 ‰ respectively, significantly different values compared to those reported here. Similarly, Fackrell et al. (2020) used a 2-year collection on West Hawai‘i to determine a LMWL with a slope of 7.65 ‰/‰ and an intercept of 15.25 ‰. While the former is comparable to what was reported in Table 3, the latter is significantly higher. One might argue that different parts of different islands experience different climatic conditions, such as evapotranspiration, temperature, and relative humidity, and these differences are reflected in the LMWLs. However, Tachera et al. (2021) recently determined a LMWL for a similar area to that considered by Fackrell et al. (2020) and found a significantly higher slope (8.14 ‰/‰) and a lower intercept (12.83 ‰).

Discussing seasonal variations of deuterium excess naturally leads one to wonder what is the interannual variability of δ^{18}O and δ^{2}H values in Hawai‘i. In their analysis of rainwater isotopic composition collected on Hawai‘i Island, Tachera et al. (2021) determined a different LMWL than that Fackrell et al. (2020) had produced from data collected in the same area only a few years before. A linear interpolation of the isotopic data in this manuscript gave a LMWL that was comparable to the one computed by Dores et al. (2020) on the island of O‘ahu, but, on the other hand, Table 3 illustrates how subsampling data could give rise to LMWLs with very different characteristics.

In order to gain a better appreciation of the intraseasonal variability of the rainfall isotopic composition in Hawai‘i, Figure 10a and 10b represent the isotopic abundances recorded at the GNIP site of Hilo during the wet and the dry season, respectively. The plots show that, while rain during the dry season tends to have a more consistent isotopic composition throughout the years of data collection, rain during the wet season shows significant differences: although with some exceptions, years in the second part of the collection tend to have lower δ^{18}O and δ^{2}H values than those in the first part. Figures 10c and 10d show deuterium excess as a function of δ^{18}O values during the wet and dry season, respectively. Rainfall with lower δ^{18}O and δ^{2}H values appears to have slightly higher deuterium excess than that with higher δ^{18}O and δ^{2}H values.

These figures suggest a significant interannual variability of rainfall isotopic composition during the wet season, and only a modest variability for dry-season precipitation. In turn, based on the prior discussion, the variability during wet-season months is

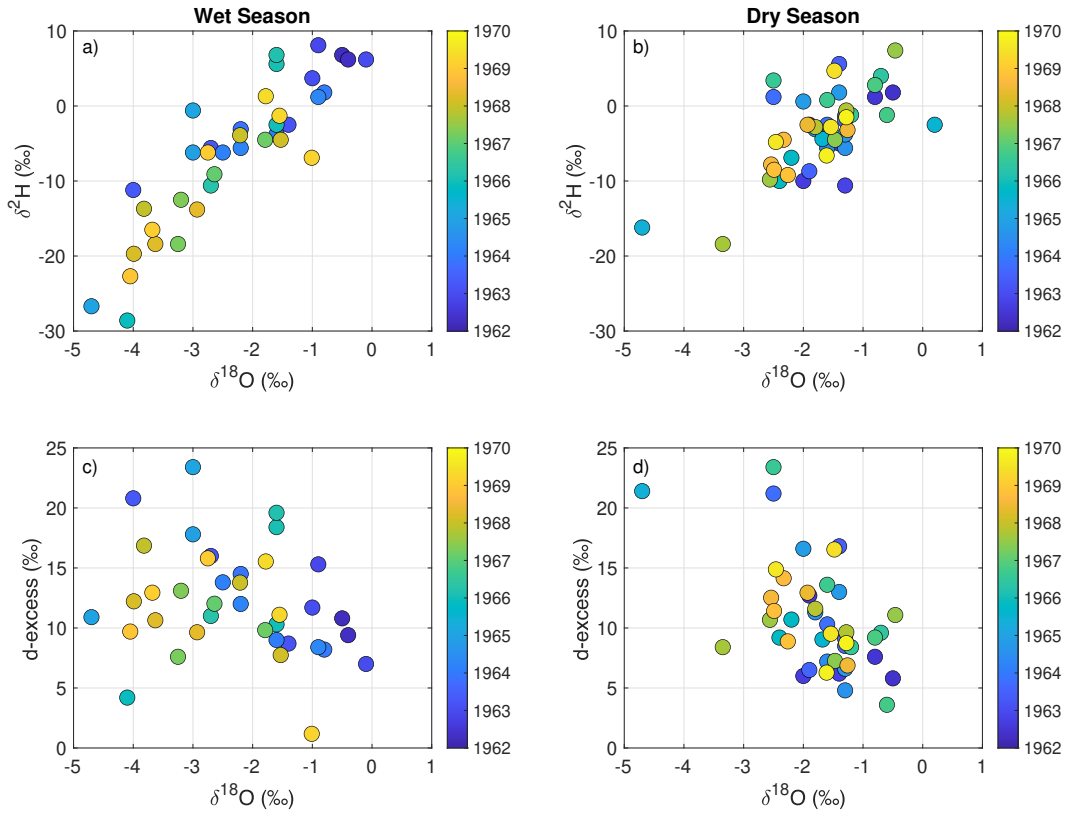

Figure 10. δ^{18}O values and deuterium excess for wet season (a,c) and dry season (b,d) shown as a function of δ^2H values for the GNIP data at Hilo. Colors reflect the year and the month when data were collected.

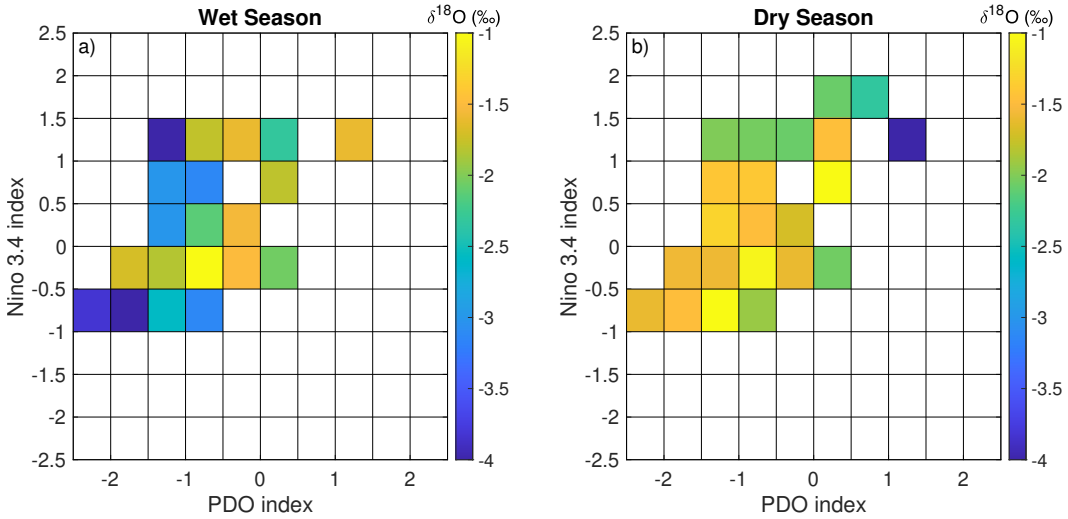

Figure 11. Average δ^{18}O for wet-season (a) and dry-season (b) rainfall GNIP data grouped based on the Niño 3.4 and PDO indices at the time when data were collected.

interpreted as due to changes in the kinds of systems that bring rainfall to Hawai'i: years with lower δ^{18}O and δ^{2}H values in wet-season rainfall are characterized by more synoptic systems, like Kona lows and cold fronts. This is also consistent with the fact that wet seasons with lower rainfall δ^{18}O and δ^{2}H values are also associated with less accumulated precipitation (not shown).

Another way of exploring the interannual variability of rainfall isotopic composition is through large-scale modes of variability, such as ENSO and the PDO, which have been shown to influence precipitation in Hawai'i (Chu & Chen, 2005). Figure 11a and 11b show average δ^{18}O values for the wet and dry season, respectively, as functions of the Niño 3.4 index (*The Climate Data Guide: Nino SST Indices (Nino 1+2, 3, 3.4, 4; ONI and TNI).*, 2021) and the NCEI PDO index (*NCEI PDO Index*, 2021). The figure suggests a possible correlation between the isotopic composition of rainfall in the wet season and the PDO, with positive phases being associated with higher δ^{18}O and δ^{2}H values. In the case of wet-season rainfall, there does not appear to be a strong correlation with Niño 3.4 index. For the dry season, on the other hand, there appears to be some correlation with ENSO, with El Niño phases being associated with more lower rainfall δ^{18}O and δ^{2}H values, but not so much with respect to the PDO. The above analysis is not meant to show rigorous evidence of a clear relationship between rainfall isotopes and ENSO or the PDO, but, merely to provide a suggestion that such a relationship might exist, and more work is needed. This would be a particularly significant finding, for example, since most of the data collection in Hawai'i that has been used to compute LMWLs and estimate aquifer recharge times is typically limited to one or two years. As Putman et al. (2019) recently pointed out, however, the correct determination of a LMWL in any particular region requires a collection on time scales at least as long as those of the processes controlling the variability. In the case of Hawai'i, this could imply the necessity of time series that span multiple years, possibly decades.

The increased collection frequency of the data presented in this manuscript represents an improvement with respect to data previously collected in Hawai'i, and it allows a clearer understanding of the isotopic composition and the origin of the systems responsible for precipitation on the islands. At the same time, there are three main limitations to this study. The first is that weekly collections might not be sufficient to make the data useful for process-based studies, for example to determine rain evaporation frac-

tion, or to assess what causes differences in the isotopic composition of trade-wind rainfall. Another limitation is that the network of sites is quite spatially limited and, given how much δ^{18}O and δ^{2}H values as well as deuterium excess can vary within the network, it leaves the open question of the spatial variability across the island of O‘ahu and, more generally, the Hawaiian Archipelago. Finally, the interannual variability suggests that even a 2-year collection might be insufficient to obtain a clear picture of rainfall water isotopic composition in Hawai‘i. Maintaining a long-time data collection over an extended region is very challenging, particularly at this historic time, but efforts are underway to overcome the limitations and increase the potential of the isotope network in Hawai‘i that has been established.

5 Conclusions

The δ^{18}O and δ^{2}H values have long been used in climate science to study, for example, past conditions on Earth, the groundwater hydrology in a given location, or, particularly in recent times, atmospheric processes and dynamics. In Hawai‘i, the water isotopic composition has been measured at different times, but most data were either collected at a time when other meteorological data were not available, or at a frequency that was too coarse to allow for a clear interpretation of the signal in terms of the weather systems responsible for rainfall. Here, a new dataset of rainfall δ^{18}O and δ^{2}H values is presented based on 2-year collections that started on the island of O‘ahu in 2019, proceeded at nearly-weekly frequency, and is still ongoing.

Compared to previous datasets, the increased frequency used for this study allowed for stronger constraints on the isotopic composition of the precipitating systems that affect the Hawaiian islands. Kona lows, subtropical storms that happen predominantly during the wet season, appear to be responsible for the lowest δ^{18}O and δ^{2}H values in rainfall. On the other hand, precipitation from cold fronts, another example of wet-season synoptic systems, presented higher values, and trade-wind showers produced rainfall with the highest δ^{18}O and δ^{2}H values. The isotopic composition of rainfall was found to be relatively similar across the network, except for the southernmost sites, where rain tended to have higher δ^{18}O and δ^{2}H values and a lower deuterium excess than the other sites, particularly during the dry season. This was interpreted as due to rain evaporation that happens as precipitating systems move across the island and encounter much drier conditions below cloud base on the leeward side, away from the Ko‘olau Range.

The data also showed a significant seasonal cycle in the deuterium excess measured at all five sites. Using trajectory analysis, the difference between wet- and dry-season deuterium excess was explained in terms of the origins of the air masses that are responsible for precipitation: during the winter months, air tends to originate at greater latitudes over the Central/West North Pacific, whereas during the summer months, air originates near the quasi-stationary high-pressure center northeast of the Hawaiian islands. Because deuterium excess in water vapor is related to SST and relative humidity at the source, differences between the two parts of the basin where rain originates were hypothesized to give rise to air masses with different deuterium excesses, which, ultimately, would manifest themselves as differences in the deuterium excess of rainfall.

Finally, the LMWL was computed and compared to previous LMWLs determined on O‘ahu and on other Hawaiian islands. Through simple sub-sampling of the data, it was shown that the LMWL is highly sensitive to the periods chosen to compute it. In order to provide a better assessment of the interannual variability of rainfall δ^{18}O and δ^{2}H values in Hawai‘i, the GNIP data from Hilo were examined. The analysis showed significant variations in the isotopic composition of wet-season rainfall and more modest variations during the dry season. The data were then compared with PDO and ENSO indices, and it was shown that wet-season rainfall shows some correlation with the for-

mer, whereas dry-season rainfall appears correlated with the latter. A much longer collection, however, is needed in order to provide more robust results.

Acknowledgments

We would like to express our gratitude to the staff of the Lyon Arboretum for granting us the permission to collect water on their grounds, and for working with us during the COVID-19 pandemic, even at times when the arboretum was closed to the public. We would also like to thank Creighton Litton, John Bravender, Nicole C. Popp, and Jan Reichelderfer for generously agreeing to help in collecting weekly rainfall samples. The data collection would have been impossible without all the passion and hard work that undergraduate students in the Department of Atmospheric Sciences Britt Seifert, Eleanore Law, and John (Jack) Fast put into this project, and to them goes our most heartfelt gratitude. The technical support and advanced computing resources from University of Hawai'i Information Technology Services – Cyberinfrastructure, funded in part by the National Science Foundation MRI award number 1920304, are also gratefully acknowledged. Finally, we want to thank Ryan Longman, Thomas Giambelluca, Yin-Phan Tsang, and Peter Huybers for enlightening discussions. G.T. was partially supported by the National Science Foundation Grant AGS-1945972. The undergraduate students and the equipment purchased for this project were supported by the Undergraduate Research Opportunities Program at the University of Hawai'i at Mānoa. The data used in this paper are available at (link to a Zenodo repository will be provided upon acceptance of the paper). This is SOEST contribution number (the number will be provided upon acceptance).

References

Adkison, C., Cooper-Norris, C., Patankar, R., & Moore, G. W. (2020). Using high-frequency water vapor isotopic measurements as a novel method to partition daily evapotranspiration in an oak woodland. *Water*, *12*(11). Retrieved from https://www.mdpi.com/2073-4441/12/11/2967 doi: 10.3390/w12112967

Aemisegger, F., Pfahl, S., Sodemann, H., Lehner, I., Seneviratne, S. I., & Wernli, H. (2014). Deuterium excess as a proxy for continental moisture recycling and plant transpiration. *Atmospheric Chemistry and Physics*, *14*(8), 4029–4054. Retrieved from https://acp.copernicus.org/articles/14/4029/2014/ doi: 10.5194/acp-14-4029-2014

Araguás-Araguás, L., Froehlich, K., & Rozanski, K. (2000). Deuterium and oxygen-18 isotope composition of precipitation and atmospheric moisture. *Hydrological Processes*, *14*(8), 1341-1355. Retrieved from https://onlinelibrary.wiley.com/doi/abs/10.1002/1099-1085%2820000615%2914%3A8%3C1341%3A%3AAID-HYP983%3E3.0.CO%3B2-Z doi: https://doi.org/10.1002/1099-1085(20000615)14:8⟨1341::AID-HYP983⟩3.0.CO;2-Z

Aron, P. G., Poulsen, C. J., Fiorella, R. P., & Matheny, A. M. (2019). Stable water isotopes reveal effects of intermediate disturbance and canopy structure on forest water cycling. *Journal of Geophysical Research: Biogeosciences*, *124*(10), 2958-2975. Retrieved from https://agupubs.onlinelibrary.wiley.com/doi/abs/10.1029/2019JG005118 doi: https://doi.org/10.1029/2019JG005118

Bailey, A., Toohey, D., & Noone, D. (2013). Characterizing moisture exchange between the hawaiian convective boundary layer and free troposphere using stable isotopes in water. *Journal of Geophysical Research: Atmospheres*, *118*(15), 8208-8221. Retrieved from https://agupubs.onlinelibrary.wiley.com/doi/abs/10.1002/jgrd.50639 doi: 10.1002/jgrd.50639

Bar-Matthews, M., Ayalon, A., & Kaufman, A. (1997). Late quaternary paleoclimate in the eastern mediterranean region from stable isotope analysis of speleothems at soreq cave, israel. *Quaternary Research*, *47*(2), 155-168.

Retrieved from https://www.sciencedirect.com/science/article/pii/S0033589497918834 doi: https://doi.org/10.1006/qres.1997.1883

Barras, V., & Simmonds, I. (2009). Observation and modeling of stable water isotopes as diagnostics of rainfall dynamics over southeastern australia. *Journal of Geophysical Research: Atmospheres*, *114*(D23). Retrieved from https://agupubs.onlinelibrary.wiley.com/doi/abs/10.1029/2009JD012132 doi: https://doi.org/10.1029/2009JD012132

Beilman, D. W., Massa, C., Nichols, J. E., Elison Timm, O., Kallstrom, R., & Dunbar-Co, S. (2019). Dynamic holocene vegetation and north pacific hydroclimate recorded in a mountain peatland, moloka'i, hawai'i. *Frontiers in Earth Science*, *7*, 188. Retrieved from https://www.frontiersin.org/article/10.3389/feart.2019.00188 doi: 10.3389/feart.2019.00188

Cai, M. Y., Wang, L., Parkes, S. D., Strauss, J., McCabe, M. F., Evans, J. P., & Griffiths, A. D. (2015). Stable water isotope and surface heat flux simulation using isolsm: Evaluation against in-situ measurements. *Journal of Hydrology*, *523*, 67-78. Retrieved from https://www.sciencedirect.com/science/article/pii/S0022169415000360 doi: https://doi.org/10.1016/j.jhydrol.2015.01.019

Cao, G., Giambelluca, T. W., Stevens, D. E., & Schroeder, T. A. (2007). Inversion variability in the hawaiian trade wind regime. *Journal of Climate*, *20*(7), 1145 - 1160. Retrieved from https://journals.ametsoc.org/view/journals/clim/20/7/jcli4033.1.xml doi: 10.1175/JCLI4033.1

Chu, P.-S., & Chen, H. (2005). Interannual and interdecadal rainfall variations in the hawaiian islands. *Journal of Climate*, *18*(22), 4796 - 4813. Retrieved from https://journals.ametsoc.org/view/journals/clim/18/22/jcli3578.1.xml doi: 10.1175/JCLI3578.1

The climate data guide: Nino sst indices (nino 1+2, 3, 3.4, 4; oni and tni). (2021). https://climatedataguide.ucar.edu/climate-data/nino-sst-indices-nino-12-3-34-4-oni-and-tni.

Cluett, A. A., & Thomas, E. K. (2020). Resolving combined influences of inflow and evaporation on western greenland lake water isotopes to inform paleoclimate inferences. *Journal of Paleolimnology*, *63*(4), 251–268. Retrieved from https://doi.org/10.1007/s10933-020-00114-4 doi: 10.1007/s10933-020-00114-4

Craig, H. (1961). Isotopic variations in meteoric waters. *Science*, *133*(3465), 1702-1703.

Cruz, F. W., Karmann, I., Viana, O., Burns, S. J., Ferrari, J. A., Vuille, M., ... Moreira, M. Z. (2005). Stable isotope study of cave percolation waters in subtropical brazil: Implications for paleoclimate inferences from speleothems. *Chemical Geology*, *220*(3), 245-262. Retrieved from https://www.sciencedirect.com/science/article/pii/S0009254105001506 doi: https://doi.org/10.1016/j.chemgeo.2005.04.001

Dahinden, F., Aemisegger, F., Wernli, H., Schneider, M., Diekmann, C. J., Ertl, B., ... Pfahl, S. (2021). Disentangling different moisture transport pathways over the eastern subtropical north atlantic using multi-platform isotope observations and high-resolution numerical modelling. *Atmospheric Chemistry and Physics Discussions*, *2021*, 1–49. Retrieved from https://acp.copernicus.org/preprints/acp-2021-269/ doi: 10.5194/acp-2021-269

Dansgaard, W. (1964). Stable isotopes in precipitation. *Tellus*, *16*(4), 436-468. Retrieved from https://onlinelibrary.wiley.com/doi/abs/10.1111/j.2153-3490.1964.tb00181.x doi: 10.1111/j.2153-3490.1964.tb00181.x

Dawson, T. E., Mambelli, S., Plamboeck, A. H., Templer, P. H., & Tu, K. P. (2002, 2021/03/01/). Stable isotopes in plant ecology. , *33*, 507–559. Retrieved from http://www.jstor.org/stable/3069272

Delmotte, M., Masson, V., Jouzel, J., & Morgan, V. I. (2000). A seasonal deuterium excess signal at law dome, coastal eastern antarctica: A southern ocean signature. *Journal of Geophysical Research: Atmospheres*, *105*(D6), 7187-7197.

Dores, D., Glenn, C. R., Torri, G., Whittier, R. B., & Popp, B. N. (2020). Implications for groundwater recharge from stable isotopic composition of precipitation in hawai'i during the 2017–2018 la niña. *Hydrological Processes*, *34*(24), 4675-4696. Retrieved from `https://onlinelibrary.wiley.com/doi/abs/10.1002/hyp.13907` doi: https://doi.org/10.1002/hyp.13907

Draxler, R., & Hess, G. (1998, 12). An overview of the hysplit4 modeling system for trajectories, dispersion, and deposition. *Australian Meteorological Magazine*, *47*, 295-308.

Ehleringer, J. R., & Dawson, T. E. (1992). Water uptake by plants: perspectives from stable isotope composition. *Plant, Cell & Environment*, *15*(9), 1073-1082. Retrieved from `https://onlinelibrary.wiley.com/doi/abs/10.1111/j.1365-3040.1992.tb01657.x` doi: https://doi.org/10.1111/j.1365-3040.1992.tb01657.x

Evaristo, J., McDonnell, J. J., Scholl, M. A., Bruijnzeel, L. A., & Chun, K. P. (2016). Insights into plant water uptake from xylem-water isotope measurements in two tropical catchments with contrasting moisture conditions. *Hydrological Processes*, *30*(18), 3210-3227. Retrieved from `https://onlinelibrary.wiley.com/doi/abs/10.1002/hyp.10841` doi: https://doi.org/10.1002/hyp.10841

Fackrell, J. K., Glenn, C. R., Thomas, D., Whittier, R., & Popp, B. N. (2020). Stable isotopes of precipitation and groundwater provide new insight into groundwater recharge and flow in a structurally complex hydrogeologic system: West hawai'i, usa. *Hydrogeology Journal*, *28*(4), 1191–1207. Retrieved from `https://doi.org/10.1007/s10040-020-02143-9` doi: 10.1007/s10040-020-02143-9

Galewsky, J. (2018). Using stable isotopes in water vapor to diagnose relationships between lower-tropospheric stability, mixing, and low-cloud cover near the island of hawaii. *Geophysical Research Letters*, *45*(1), 297-305. Retrieved from `https://agupubs.onlinelibrary.wiley.com/doi/abs/10.1002/2017GL075770` doi: 10.1002/2017GL075770

Galewsky, J., Steen-Larsen, H. C., Field, R. D., Worden, J., Risi, C., & Schneider, M. (2016). Stable isotopes in atmospheric water vapor and applications to the hydrologic cycle. *Reviews of Geophysics*, *54*(4), 809-865. Retrieved from `https://agupubs.onlinelibrary.wiley.com/doi/abs/10.1002/2015RG000512` doi: 10.1002/2015RG000512

Galewsky, J., Strong, M., & Sharp, Z. D. (2007). Measurements of water vapor d/h ratios from mauna kea, hawaii, and implications for subtropical humidity dynamics. *Geophysical Research Letters*, *34*(22). Retrieved from `https://agupubs.onlinelibrary.wiley.com/doi/abs/10.1029/2007GL031330` doi: 10.1029/2007GL031330

Giambelluca, T. W., Chen, Q., Frazier, A. G., Price, J. P., Chen, Y.-L., Chu, P.-S., ... Delparte, D. M. (2013). Online rainfall atlas of hawai'i. *Bulletin of the American Meteorological Society*, *94*(3), 313 - 316. Retrieved from `https://journals.ametsoc.org/view/journals/bams/94/3/bams-d-11-00228.1.xml` doi: 10.1175/BAMS-D-11-00228.1

Gingerich, S., & Oki, D. S. (2000). Ground water in hawaii. *U.S. Geological Survey. p. 6.*.

Gröning, M., Lutz, H., Roller-Lutz, Z., Kralik, M., Gourcy, L., & Pöltenstein, L. (2012). A simple rain collector preventing water re-evaporation dedicated for 18o and 2h analysis of cumulative precipitation samples. *Journal of Hydrology*, *448-449*, 195-200. Retrieved from `https://www.sciencedirect.com/science/article/pii/S0022169412003411` doi: https://doi.org/10.1016/

j.jhydrol.2012.04.041

Grossiord, C., Sevanto, S., Dawson, T. E., Adams, H. D., Collins, A. D., Dickman, L. T., ... McDowell, N. G. (2017). Warming combined with more extreme precipitation regimes modifies the water sources used by trees. *New Phytologist*, *213*(2), 584-596. Retrieved from https://nph.onlinelibrary.wiley.com/doi/abs/10.1111/nph.14192 doi: https://doi.org/10.1111/nph.14192

Guan, H., Zhang, X., Skrzypek, G., Sun, Z., & Xu, X. (2013). Deuterium excess variations of rainfall events in a coastal area of south australia and its relationship with synoptic weather systems and atmospheric moisture sources. *Journal of Geophysical Research: Atmospheres*, *118*(2), 1123-1138. Retrieved from https://agupubs.onlinelibrary.wiley.com/doi/abs/10.1002/jgrd.50137 doi: https://doi.org/10.1002/jgrd.50137

Gupta, P., Noone, D., Galewsky, J., Sweeney, C., & Vaughn, B. H. (2009). Demonstration of high-precision continuous measurements of water vapor isotopologues in laboratory and remote field deployments using wavelength-scanned cavity ring-down spectroscopy (ws-crds) technology. *Rapid Communications in Mass Spectrometry*, *23*(16), 2534-2542. Retrieved from https://onlinelibrary.wiley.com/doi/abs/10.1002/rcm.4100 doi: https://doi.org/10.1002/rcm.4100

Hahn, M., Jacobs, S. R., Breuer, L., Rufino, M. C., & Windhorst, D. (2021). Variability in tree water uptake determined with stable water isotopes in an african tropical montane forest. *Ecohydrology*, *n/a*(n/a), e2278. Retrieved from https://onlinelibrary.wiley.com/doi/abs/10.1002/eco.2278 doi: https://doi.org/10.1002/eco.2278

Hartley, T. M., & Chen, Y.-L. (2010). Characteristics of summer trade wind rainfall over oahu. *Weather and Forecasting*, *25*(6), 1797 - 1815. Retrieved from https://journals.ametsoc.org/view/journals/wefo/25/6/2010waf2222328_1.xml doi: 10.1175/2010WAF2222328.1

Hersbach, H., Bell, W., Berrisford, P., Horányi, A., J., M.-S., Nicolas, J., ... Dee, D. (2019, 04). Global reanalysis: goodbye era-interim, hello era5. , 17-24. Retrieved from https://www.ecmwf.int/node/19027 doi: 10.21957/vf291hehd7

Hurley, J. V., Galewsky, J., Worden, J., & Noone, D. (2012). A test of the advection-condensation model for subtropical water vapor using stable isotopologue observations from mauna loa observatory, hawaii. *Journal of Geophysical Research: Atmospheres*, *117*(D19). Retrieved from https://agupubs.onlinelibrary.wiley.com/doi/abs/10.1029/2012JD018029 doi: 10.1029/2012JD018029

IAEA/WMO. (2021). Global network of isotopes in precipitation. the gnip database. *Accessible at: http://www.iaea.org/water*.

Jouzel, J., Stiévenard, M., Johnsen, S., Landais, A., Masson-Delmotte, V., Sveinbjornsdottir, A., ... White, J. (2007). The grip deuterium-excess record. *Quaternary Science Reviews*, *26*(1), 1-17. Retrieved from https://www.sciencedirect.com/science/article/pii/S0277379106002575 doi: https://doi.org/10.1016/j.quascirev.2006.07.015

Kelly, J. L., & Glenn, C. R. (2015). Chlorofluorocarbon apparent ages of groundwaters from west hawaii, usa. *Journal of Hydrology*, *527*, 355-366. Retrieved from https://www.sciencedirect.com/science/article/pii/S0022169415003285 doi: https://doi.org/10.1016/j.jhydrol.2015.04.069

Kodama, K., & Barnes, G. M. (1997). Heavy rain events over the south-facing slopes of hawaii: Attendant conditions. *Weather and Forecasting*, *12*(2), 347 - 367. Retrieved from https://journals.ametsoc.org/view/journals/wefo/12/2/1520-0434_1997_012_0347_hreots_2_0_co_2.xml doi: 10.1175/1520-0434(1997)012⟨0347:HREOTS⟩2.0.CO;2

Kodama, K. R., & Businger, S. (1998). Weather and forecasting challenges in the pacific region of the national weather service. *Weather and Forecasting*, *13*(3), 523 - 546. Retrieved from https://journals.ametsoc.org/view/journals/wefo/13/3/1520-0434_1998_013_0523_wafcit_2_0_co_2.xml doi: 10.1175/1520-0434(1998)013⟨0523:WAFCIT⟩2.0.CO;2

Kontakiotis, G. (2016). Late quaternary paleoenvironmental reconstruction and paleoclimatic implications of the aegean sea (eastern mediterranean) based on paleoceanographic indexes and stable isotopes. *Quaternary International*, *401*, 28-42. Retrieved from https://www.sciencedirect.com/science/article/pii/S1040618215007156 (Implications for Late Quaternary Sea Level Changes on the Mediterranean and Black Sea Coasts - MEDBLACKS2014) doi: https://doi.org/10.1016/j.quaint.2015.07.039

Kopec, B. G., Feng, X., Posmentier, E. S., & Sonder, L. J. (2019). Seasonal deuterium excess variations of precipitation at summit, greenland, and their climatological significance. *Journal of Geophysical Research: Atmospheres*, *124*(1), 72-91. Retrieved from https://agupubs.onlinelibrary.wiley.com/doi/abs/10.1029/2018JD028750 doi: https://doi.org/10.1029/2018JD028750

Lai, C.-T., & Ehleringer, J. R. (2011). Deuterium excess reveals diurnal sources of water vapor in forest air. *Oecologia*, *165*(1), 213–223. Retrieved from https://doi.org/10.1007/s00442-010-1721-2 doi: 10.1007/s00442-010-1721-2

LeGrande, A. N., & Schmidt, G. A. (2009). Sources of holocene variability of oxygen isotopes in paleoclimate archives. *Climate of the Past*, *5*(3), 441–455. Retrieved from https://cp.copernicus.org/articles/5/441/2009/ doi: 10.5194/cp-5-441-2009

Longman, R. J., Timm, O. E., Giambelluca, T. W., & Kaiser, L. (2021). A 20-year analysis of disturbance-driven rainfall on o'ahu, hawai'i. *Monthly Weather Review*, *149*(6), 1767 - 1783. Retrieved from https://journals.ametsoc.org/view/journals/mwre/149/6/MWR-D-20-0287.1.xml doi: 10.1175/MWR-D-20-0287.1

Lovelock, C. E., Reef, R., & Ball, M. C. (2017). Isotopic signatures of stem water reveal differences in water sources accessed by mangrove tree species. *Hydrobiologia*, *803*(1), 133–145. Retrieved from https://doi.org/10.1007/s10750-017-3149-8 doi: 10.1007/s10750-017-3149-8

Mantua, N. J., Hare, S. R., Zhang, Y., Wallace, J. M., & Francis, R. C. (1997). A pacific interdecadal climate oscillation with impacts on salmon production*. *Bulletin of the American Meteorological Society*, *78*(6), 1069 - 1080. Retrieved from https://journals.ametsoc.org/view/journals/bams/78/6/1520-0477_1997_078_1069_apicow_2_0_co_2.xml doi: 10.1175/1520-0477(1997)078⟨1069:APICOW⟩2.0.CO;2

Marshall, J. D., Brooks, J. R., & Lajtha, K. (2007). Sources of variation in the stable isotopic composition of plants. In *Stable isotopes in ecology and environmental science* (p. 22-60). John Wiley Sons, Ltd. Retrieved from https://onlinelibrary.wiley.com/doi/abs/10.1002/9780470691854.ch2 doi: https://doi.org/10.1002/9780470691854.ch2

Massa, C., Beilman, D. W., Nichols, J. E., & Timm, O. E. (2021). Central pacific hydroclimate over the last 45,000 years: Molecular-isotopic evidence from leaf wax in a hawaii peatland. *Quaternary Science Reviews*, *253*, 106744. Retrieved from https://www.sciencedirect.com/science/article/pii/S027737912030706X doi: https://doi.org/10.1016/j.quascirev.2020.106744

Masson-Delmotte, V., Jouzel, J., Landais, A., Stievenard, M., Johnsen, S. J., White, J. W. C., ... Fuhrer, K. (2005). Grip deuterium excess reveals rapid and orbital-scale changes in greenland moisture origin. *Science*, *309*(5731), 118-121.

Merlivat, L., & Jouzel, J. (1979). Global climatic interpretation of the deuterium-oxygen 18 relationship for precipitation. *Journal of Geophys-*

ical Research: Oceans, *84*(C8), 5029-5033. Retrieved from https://agupubs.onlinelibrary.wiley.com/doi/abs/10.1029/JC084iC08p05029 doi: https://doi.org/10.1029/JC084iC08p05029

Ncei pdo index. (2021). https://www.ncdc.noaa.gov/teleconnections/pdo/.

Noone, D., Galewsky, J., Sharp, Z. D., Worden, J., Barnes, J., Baer, D., ... Wright, J. S. (2011). Properties of air mass mixing and humidity in the subtropics from measurements of the d/h isotope ratio of water vapor at the mauna loa observatory. *Journal of Geophysical Research: Atmospheres*, *116*(D22). Retrieved from https://agupubs.onlinelibrary.wiley.com/doi/abs/10.1029/2011JD015773 doi: 10.1029/2011JD015773

Opel, T., Meyer, H., Wetterich, S., Laepple, T., Dereviagin, A., & Murton, J. (2018). Ice wedges as archives of winter paleoclimate: A review. *Permafrost and Periglacial Processes*, *29*(3), 199-209. Retrieved from https://onlinelibrary.wiley.com/doi/abs/10.1002/ppp.1980 doi: https://doi.org/10.1002/ppp.1980

Papritz, L., Aemisegger, F., & Wernli, H. (2021). Sources and transport pathways of precipitating waters in cold-season deep north atlantic cyclones. *Journal of the Atmospheric Sciences*. Retrieved from https://journals.ametsoc.org/view/journals/atsc/aop/JAS-D-21-0105.1/JAS-D-21-0105.1.xml doi: 10.1175/JAS-D-21-0105.1

Pfahl, S., & Sodemann, H. (2014). What controls deuterium excess in global precipitation? *Climate of the Past*, *10*(2), 771–781. Retrieved from https://cp.copernicus.org/articles/10/771/2014/ doi: 10.5194/cp-10-771-2014

Pfahl, S., & Wernli, H. (2009). Lagrangian simulations of stable isotopes in water vapor: An evaluation of nonequilibrium fractionation in the craig-gordon model. *Journal of Geophysical Research: Atmospheres*, *114*(D20). Retrieved from https://agupubs.onlinelibrary.wiley.com/doi/abs/10.1029/2009JD012054 doi: https://doi.org/10.1029/2009JD012054

Putman, A. L., Fiorella, R. P., Bowen, G. J., & Cai, Z. (2019). A global perspective on local meteoric water lines: Meta-analytic insight into fundamental controls and practical constraints. *Water Resources Research*, *55*(8), 6896-6910. Retrieved from https://agupubs.onlinelibrary.wiley.com/doi/abs/10.1029/2019WR025181 doi: https://doi.org/10.1029/2019WR025181

Rozanski, K., Araguás-Araguás, L., & Gonfiantini, R. (1993). Isotopic patterns in modern global precipitation. In *Climate change in continental isotopic records* (p. 1-36). American Geophysical Union (AGU). Retrieved from https://agupubs.onlinelibrary.wiley.com/doi/abs/10.1029/GM078p0001 doi: https://doi.org/10.1029/GM078p0001

Scholl, M. A., Giambelluca, T. W., Gingerich, S. B., Nullet, M. A., & Loope, L. L. (2007). Cloud water in windward and leeward mountain forests: The stable isotope signature of orographic cloud water. *Water Resources Research*, *43*(12). Retrieved from https://agupubs.onlinelibrary.wiley.com/doi/abs/10.1029/2007WR006011 doi: https://doi.org/10.1029/2007WR006011

Scholl, M. A., Gingerich, S. B., & Tribble, G. W. (2002). The influence of microclimates and fog on stable isotope signatures used in interpretation of regional hydrology: East maui, hawaii. *Journal of Hydrology*, *264*(1), 170-184. Retrieved from https://www.sciencedirect.com/science/article/pii/S0022169402000732 doi: https://doi.org/10.1016/S0022-1694(02)00073-2

Scholl, M. A., Ingebritsen, S. E., Janik, C. J., & Kauahikaua, J. P. (1996). Use of precipitation and groundwater isotopes to interpret regional hydrology on a tropical volcanic island: Kilauea volcano area, Hawaii. *Water Resources Research*, *32*(12), 3525–3537. doi: 10.1029/95WR02837

Simpson, R. H. (1952). Evolution of the kona storm a subtropical cyclone. *Journal of Atmospheric Sciences*, *9*(1), 24 - 35. Retrieved from https://journals.ametsoc.org/view/journals/atsc/9/1/1520-0469_1952_009_0024_eotksa

_2_0_co_2.xml doi: 10.1175/1520-0469(1952)009⟨0024:EOTKSA⟩2.0.CO;2

Sodemann, H., Masson-Delmotte, V., Schwierz, C., Vinther, B. M., & Wernli, H. (2008). Interannual variability of greenland winter precipitation sources: 2. effects of north atlantic oscillation variability on stable isotopes in precipitation. *Journal of Geophysical Research: Atmospheres*, *113*(D12). Retrieved from https://agupubs.onlinelibrary.wiley.com/doi/abs/10.1029/2007JD009416 doi: https://doi.org/10.1029/2007JD009416

State of hawaii data book. (2004). Hawaii. Dept. of Business, Economic Development and Tourism. Research and Economic Analysis Division. Statistics and Data Support Branch.

Stein, A. F., Draxler, R. R., Rolph, G. D., Stunder, B. J. B., Cohen, M. D., & Ngan, F. (2015). Noaa's hysplit atmospheric transport and dispersion modeling system. *Bulletin of the American Meteorological Society*, *96*(12), 2059 - 2077. Retrieved from https://journals.ametsoc.org/view/journals/bams/96/12/bams-d-14-00110.1.xml doi: 10.1175/BAMS-D-14-00110.1

Tachera, D. K., Lautze, N. C., Torri, G., & Thomas, D. M. (2021). Characterization of the isotopic composition and bulk ion deposition of precipitation from central to west hawaii island between 2017 and 2019. *Journal of Hydrology: Regional Studies*, *34*, 100786. Retrieved from https://www.sciencedirect.com/science/article/pii/S221458182100015X doi: https://doi.org/10.1016/j.ejrh.2021.100786

Tetzlaff, D., Buttle, J., Carey, S. K., Kohn, M. J., Laudon, H., McNamara, J. P., ... Soulsby, C. (2021). Stable isotopes of water reveal differences in plant – soil water relationships across northern environments. *Hydrological Processes*, *35*(1), e14023. Retrieved from https://onlinelibrary.wiley.com/doi/abs/10.1002/hyp.14023 doi: https://doi.org/10.1002/hyp.14023

Tillman, F. D., Oki, D. S., Johnson, A. G., Barber, L. B., & Beisner, K. R. (2014). Investigation of geochemical indicators to evaluate the connection between inland and coastal groundwater systems near kaloko-honokōhau national historical park, hawai'i. *Applied Geochemistry*, *51*, 278–292. Retrieved from https://www.sciencedirect.com/science/article/pii/S0883292714002352 doi: https://doi.org/10.1016/j.apgeochem.2014.10.003

Timofeeva, G., Treydte, K., Bugmann, H., Salmon, Y., Rigling, A., Schaub, M., ... Saurer, M. (2020, 06). How does varying water supply affect oxygen isotope variations in needles and tree rings of Scots pine? *Tree Physiology*, *40*(10), 1366-1380. Retrieved from https://doi.org/10.1093/treephys/tpaa082 doi: 10.1093/treephys/tpaa082

Trenberth, K. E. (1997). The definition of el niño. *Bulletin of the American Meteorological Society*, *78*(12), 2771 - 2778. Retrieved from https://journals.ametsoc.org/view/journals/bams/78/12/1520-0477_1997_078_2771_tdoeno_2_0_co_2.xml doi: 10.1175/1520-0477(1997)078⟨2771:TDOENO⟩2.0.CO;2

Uemura, R., Matsui, Y., Yoshimura, K., Motoyama, H., & Yoshida, N. (2008). Evidence of deuterium excess in water vapor as an indicator of ocean surface conditions. *Journal of Geophysical Research: Atmospheres*, *113*(D19). Retrieved from https://doi.org/10.1029/2008JD010209 doi: https://doi.org/10.1029/2008JD010209

U.S. Census Bureau, P. D. (2020). *Annual estimates of the resident population for the united states, regions, states, and the district of columbia: April 1, 2010 to july 1, 2020 (nst-est2020).*

Veron, S., Mouchet, M., Govaerts, R., Haevermans, T., & Pellens, R. (2019). Vulnerability to climate change of islands worldwide and its impact on the tree of life. *Scientific Reports*, *9*(1), 14471. Retrieved from https://doi.org/10.1038/s41598-019-51107-x doi: 10.1038/s41598-019-51107-x

Villiger, L., Wernli, H., Boettcher, M., Hagen, M., & Aemisegger, F. (2021). Lagrangian formation pathways of moist anomalies in the trade-wind region during the dry season: two case studies from eurec^{4}a. *Weather and Climate Dynamics Discussions*, *2021*, 1–49. Retrieved from `https://wcd.copernicus.org/preprints/wcd-2021-42/` doi: 10.5194/wcd-2021-42

Vimeux, F., Masson, V., Jouzel, J., Stievenard, M., & Petit, J. R. (1999). Glacial–interglacial changes in ocean surface conditions in the southern hemisphere. *Nature*, *398*(6726), 410–413. Retrieved from `https://doi.org/10.1038/18860` doi: 10.1038/18860

Woodruff, F., Savin, S. M., & Douglas, R. G. (1981). Miocene stable isotope record: A detailed deep pacific ocean study and its paleoclimatic implications. *Science*, *212*(4495), 665–668. Retrieved from `https://science.sciencemag.org/content/212/4495/665` doi: 10.1126/science.212.4495.665

Yao, T., Masson-Delmotte, V., Gao, J., Yu, W., Yang, X., Risi, C., ... Hou, S. (2013). A review of climatic controls on 18o in precipitation over the tibetan plateau: Observations and simulations. *Reviews of Geophysics*, *51*(4), 525-548. Retrieved from `https://agupubs.onlinelibrary.wiley.com/doi/abs/10.1002/rog.20023` doi: https://doi.org/10.1002/rog.20023

Yoshimura, K. (2015). Stable water isotopes in climatology, meteorology, and hydrology: A review. . *2*, *93*(5), 513–533. doi: 10.2151/jmsj.2015-036

Yoshimura, K., & Ichiyanagi, K. (2009). A reconsideration of seasonal variation in precipitation deuterium excess over east asia. *Journal of Japan Society of Hydrology and Water Resources*, *22*(4), 262-276.